Evaluation of water profiles at silica surfaces at 23°C, 100°C and 200°C by Zouine et al.

Günter Schell, Claudia Bucharsky, Theo Fett

KIT SCIENTIFIC WORKING PAPERS ÁÍÍ&$- ¨¨¨¨
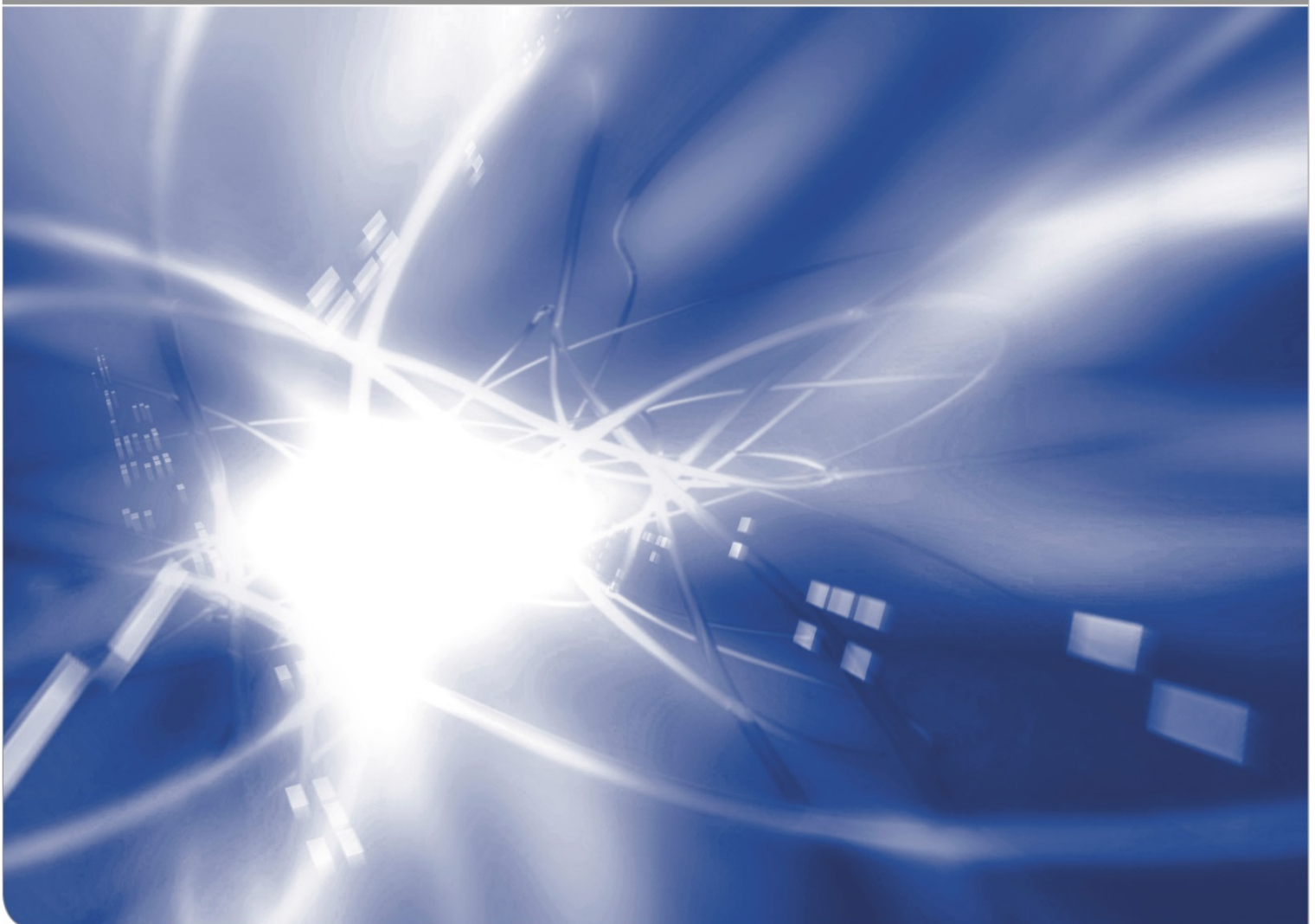
Institute for Applied Materials

Abstract

The reaction equation for the reaction between water and silica reads

$$\equiv\text{Si-O-Si}\equiv +H_2O \leftrightarrow [2\ SiOH]$$

For this reaction the equilibrium constant, k, is affected by internal swelling stresses. We investigated the behaviour of erfc-shaped distributions of the total water amount in earlier Reports. The present report is intended to evaluate more complicated water profiles. Water concentrations at silica surfaces were measured by Zouine et al. Some of their data showed deviations from the expected erfc-shape. The associated datasets were used to demonstrate the procedure of determining the local equilibrium constant and the distributions of the hydroxyl and molecular water species on irregular water distributions.

In an Appendix we discuss what could be the reason for the deviations in the distribution of the total water C_w from the erfc-shape. The occurrence of back-diffusion after aging is assumed.

Contents

1 Basic equations

Water penetrated into silica reacts with the silica network. In our Reports [1] and [2] we dealt with the shape of the water profiles at silica surfaces. We found that the equilibrium between hydroxyl $S = [\equiv\text{SiOH}]$ and molecular water $C = [\text{H}_2\text{O}]$ of the reaction

$$\equiv\text{Si-O-Si}\equiv +\text{H}_2\text{O} \leftrightarrow \equiv\text{SiOH+HOSi}\equiv \tag{1}$$

must change with the distance from the glass surface due to the compressive swelling stresses. Expressed in terms of the equilibrium constant k,

$$k = \frac{S}{C} \tag{2}$$

the equilibrium also becomes dependent on concentration and location.

Then the equilibrium constant reads according to [3]

$$k = k_0 \exp\left(-\lambda\frac{S\Delta V}{RT}\right) \tag{3}$$

with $\lambda=18.8$ GPa. The hydrostatic swelling stress is expressed by

$$\sigma_{sw,h} = -\lambda S \ . \tag{4}$$

Only erfc-shaped distributions $C_w(z)$ of the total water

$$C_w = C + \tfrac{1}{2}S \tag{5}$$

were prescribed in [2]

$$C_w = C_w(0)\,\text{erfc}\left(\frac{z}{2b}\right) \tag{6}$$

The present report is intended to evaluate more complicated water profiles. Water concentrations at silica surfaces under saturation pressure are available from an investigation by Zouine et al. [4]. For our computations we used an activation volume of $\Delta V\cong 58$ cm^3/mol as was obtained in [2] by a fitting procedure.

Some results in [4] deviate from the simple erfc-description as can be seen for measurements compiled in Fig. 1a. Figure 1b represents the same results in a normalized representation where $C(0)$ are the surface concentrations from Table 1 in [4] and additionally the concentrations are divided by the diffusion depth b at which the erfc function has the value of $\cong\frac{1}{2}$.
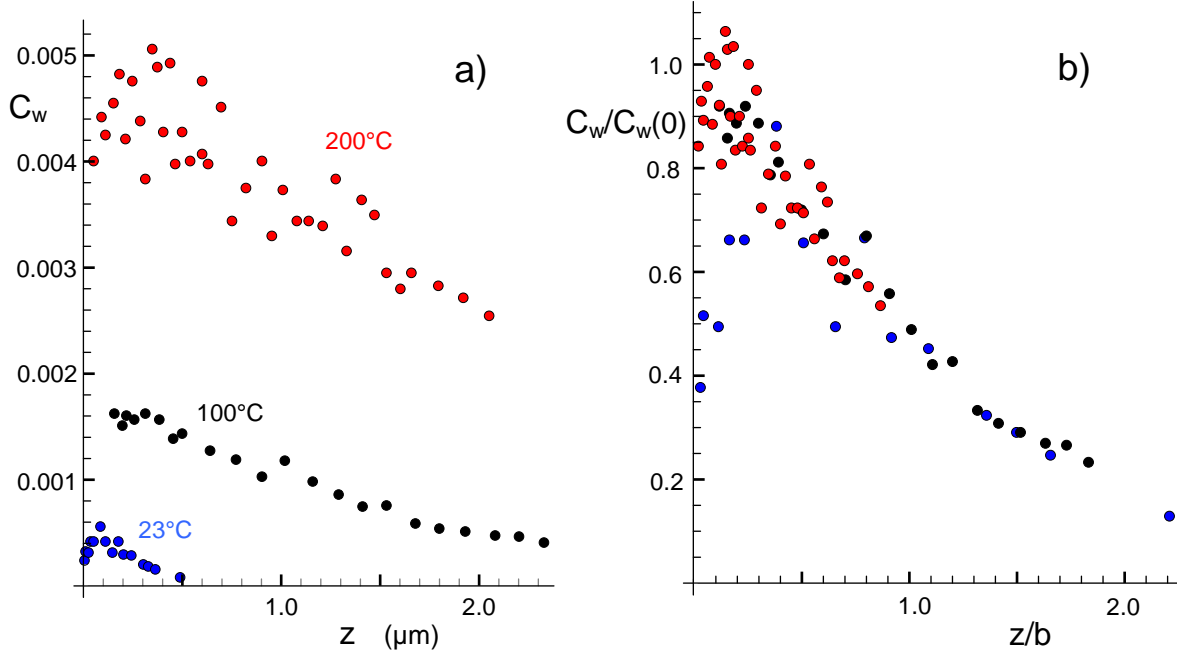
Fig. 1 Some irregular profiles a) total water content $C_w(z)$ measured by Zouine et al. [4], b) same data in normalized representation, $C_w(0)$, $C_w(z=0)$.

The equilibrium constant as a function of the measured C_w finally results from (3) in the implicit equation

$$k = k_0 \exp\left(-\frac{\lambda \Delta V}{RT} \frac{C_w}{\frac{1}{2} + \frac{1}{k}} \right) \qquad (7)$$

since k is present on the left-hand side as well as on the right-hand side in the denominator of the exponential function. From the measured values of C_w the two water species S and C can be computed via

$$C = \frac{C_w}{1 + \frac{1}{2}k}, \qquad (8)$$

$$S = \frac{17}{18} \frac{C_w}{\left(\frac{1}{2} + \frac{1}{k} \right)} \qquad (9)$$

2. Evaluation of profiles with irregular behaviour at the surface

2.1 Evaluation at 200°C

The water profiles S, C were computed via eqs.(8) and (9) and plotted in Fig. 2 together with the total water concentrations C_w as measured in [4]. The shortest distance below the surface is about $z=40$-50 nm.
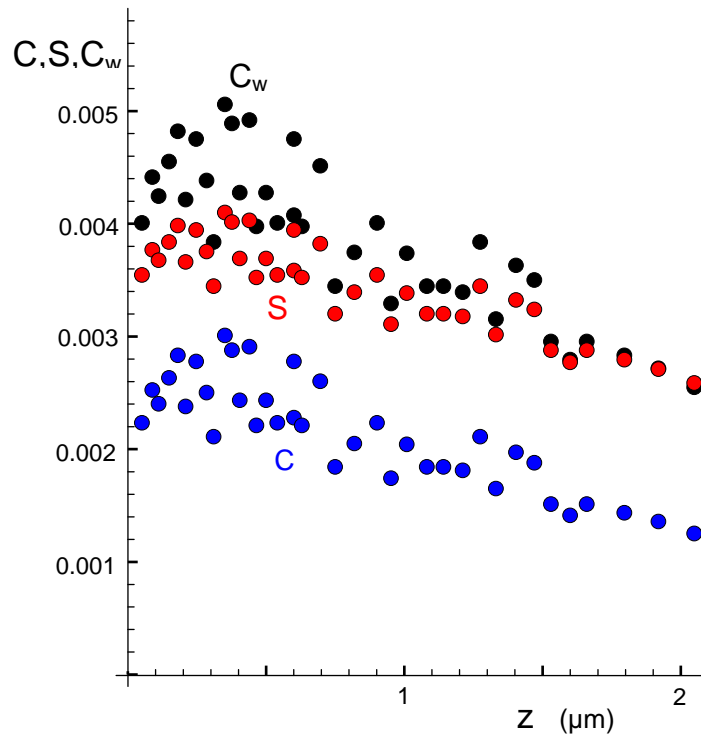
Fig. 2 Water species *S* and *C*, derived from the measurements of total water, C_w, for soaking at 200°C.

2.2 Evaluation at 100°C

The profiles obtained after a soaking time of 1319h are shown in Fig. 3. Unfortunately, there are no data available for $z<170$nm.
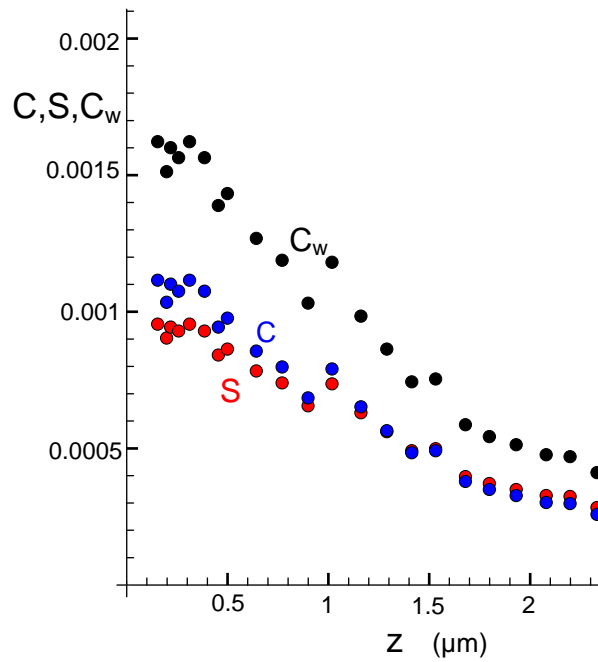
Fig. 3 Water species *S* and *C*, derived from the measurements of total water, C_w, for soaking at 100°C.

2.3 Evaluation at 23°C

Finally, Fig. 4 shows the profiles at room temperature hydrated for about 15000h in humid air. At distances of 0<z<170nm, the water concentrations are significantly lower than expected from eq.(6). In this range, the distribution no longer follows eq.(6). Regarding the low concentration near the surface, the authors of [4] note:

"In the 23°C/air profile the near surface data points lie lower than to be expected. The reason for this is not clear. However, it seemed justified to omit these data points in fitting the profile."
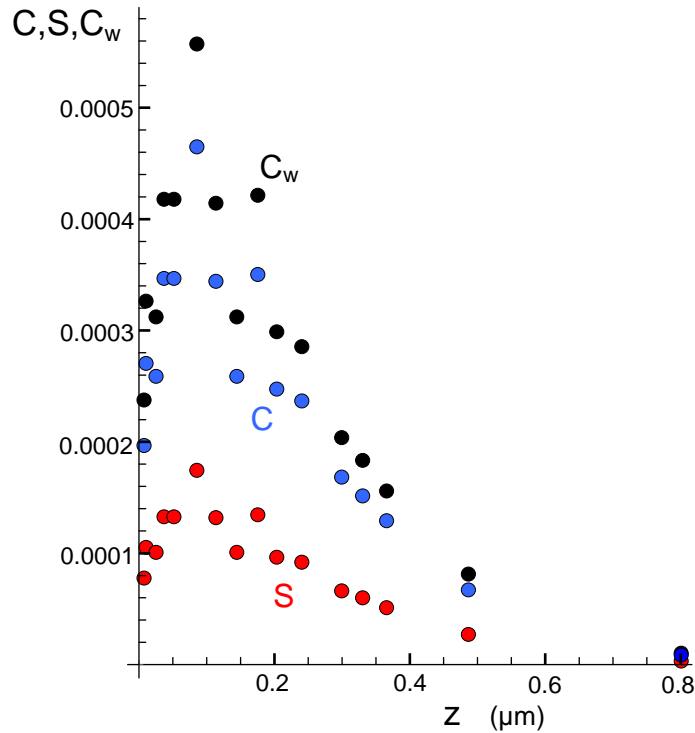
Fig. 4 Water species S and C, derived from the measurements of total water, C_w, for soaking at room temperature 23°C.

Remarks:

- In [1] we found that the hydroxyl water profile $S(z)$ for small depth z must decrease with respect to the shape of the total water concentration as obtained by the nuclear reaction analysis (NRA). This was concluded for a C_w-distribution of type eq.(6). From Figs. 2-4, we can see that the same effect occurs also for different types of $C_w(z)$. This makes it understandable that the concentration curves of the two water species S and C deviate from the curve of the total water concentration C_w, but does not explain why C_w itself shows the really unexpected distributions.

- It is obvious that the equilibrium constant varies in a water diffusion zone where C_w varies with depth and an average value $\bar{k}$ over the depth profile

4

$$k = \frac{\overline{S}}{\overline{C}} = \frac{\int S(z)dz}{\int C(z)dz} \qquad (10)$$

according to [1], determined by measurements of Wiederhorn et al. [5]. Figure 5 shows the local distribution of the equilibrium constant $k(z)$ as the circles. The dash-dotted lines indicate the average values according to eq.(10).

- In the Appendix, we want to investigate whether back-diffusion may occur during the storage until the measurement, which is not defined in the article.
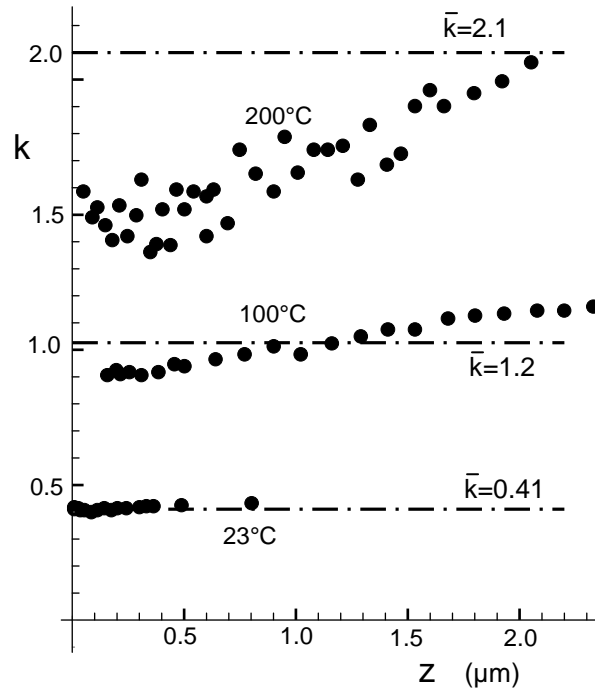
Fig. 5 Varying equilibrium constant k as a function of depth, horizontal lines: averages over the whole water zone, according to [1].

Appendix:

A probable reason for the occurrence of irregular profiles

The irregular distributions of the measurement data from Zouine et al. [4], especially those at room temperature, can be understood by back-diffusion after water or air storage, respectively.

Unfortunately, no detailed information on storage after the end of the experiment is given in [4]. It therefore remains unclear in which medium and for how long the samples were in until the subsequent NRA measurement.

Due to this circumstance, only the possibility of the effect should be addressed here, but no quantitative information should be given.

This may be illustrated here by superimposing two erfc distributions of the type

$$C_w = a_0 \operatorname{erfc}[a_1 z] + a_2 \operatorname{erfc}[a_3 z] \qquad (11)$$

the first describing diffusion during aging in the wet medium and the second describing diffusion towards the surface after aging. Zouine et al. [4] fitted the data far from the surface and thereby obtained the parameters a_0 and a_1 (introduced as curves in the original plots). Table 1 compiles these coefficients in the columns 2 and 3.

We fitted the whole data by eq.(11) and obtained the two parameters a_2 and a_3, given in columns 4 and 5. The negative parameter a_1 can be taken as an indication of a reversal of diffusion. Finally, the best fitting curves are plotted in Figs. 6a-6c.
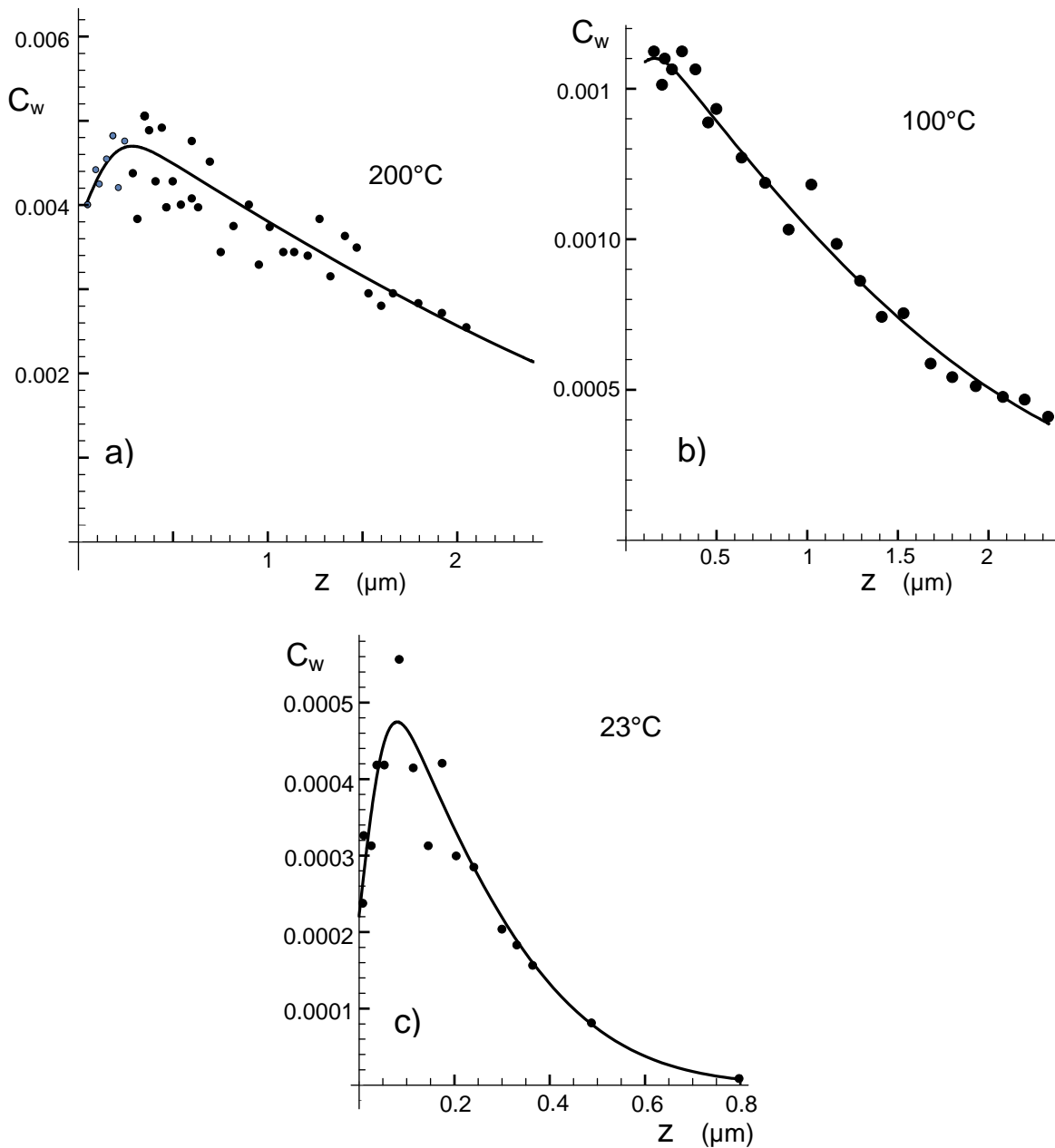
Fig. 6 Total water profiles $C_w(z)$, fitted by two superimposed erfc-functions according to eq.(11) using the parameters of Table 1.

Temperature	a_0	a_1 (μm^{-1})	a_2	a_3 (μm^{-1})
200°C	0.0052	0.2421	-0.00143	4.53
100°C	0.00177	0.377	-0.000254	5.73
23°C	0.00063	2.218	-0.00041	15.6

Table 1 Parameters for eq.(11) obtained by curve fitting to data of Figs. 6a-6c.

References

1 T. Fett, K.G. Schell, C.E. Bucharsky, Distribution of equilibrium constant *k* and hydroxyl *S* in silica surface layers, SWP **195**, 2022, ISSN: 2194-1629, Karlsruhe, KIT.

2 T. Fett, K.G. Schell, C.E. Bucharsky, Interpretation of silica-disk-tests including the effect of limited mass transfer at the surface, SWP **196**, 2022, ISSN: 2194-1629, Karlsruhe, KIT.

3 T. Fett, G. Rizzi, K.G. Schell, C.E. Bucharsky, P. Hettich, S. Wagner, M. J. Hoffmann, Consequences of hydroxyl generation by the silica/water reaction, Part I: Diffusion and Swelling, KIT Scientific Publishing, **101**(2022), Karlsruhe.

4 A. Zouine, O. Dersch, G. Walter and F. Rauch, "Diffusivity and solubility of water in silica glass in the temperature range 23-200°C," *Phys. Chem. Glass: Eur. J. Glass Sci and Tech. Pt. B*, **48** [2] 85-91 (2007).

5 S. M. Wiederhorn, F. Yi, D. LaVan, T. Fett, M.J. Hoffmann, Volume Expansion caused by Water Penetration into Silica Glass, J. Am. Ceram. Soc. **98** (2015), 78-87.